

## Article

# High-Rise Residential District Morphology Optimization for Enhancing the Green Space Cooling Effect

Feng Shi, Yuan Chen <sup>\*</sup>, Wenru Yue and Yupeng Wang 

School of Human Settlements and Civil Engineering, Xi'an Jiaotong University, Xi'an 710049, China; casperslifeng@xjtu.edu.cn (F.S.); g1059082562@gmail.com (W.Y.); wang-yupeng@xjtu.edu.cn (Y.W.)

\* Correspondence: y.chen@stu.xjtu.edu.cn

**Abstract:** Large-scale urban green spaces exert a cooling effect in cities and have great potential for optimizing the urban climate. In this study, taking the typical green space Xingfulindai in Xi'an as an example, we carried out field measurements and ENVI-met simulations of the area and the surrounding high-rise residential areas to analyze the cooling effect. The results show that the cooling effect is the strongest at night in summer seasons, spreading up to 250 m, and the cooling intensity along the downwind direction can be up to 2 °C. On this basis, a total of 16 ideal models of seven groups of high-rise residential blocks were established to analyze the effect of three morphological indices, namely, building orientation, podium ratio, and otherness with respect to the cooling effect of the green space, and a block morphology design strategy for high-rise residential areas was proposed to enhance the cooling effect of the green space. This study provides climate-adaptive optimization strategies for the construction and renewal of residential blocks.

**Keywords:** urban cool island; urban morphology; environmental evaluation; district development



**Citation:** Shi, F.; Chen, Y.; Yue, W.; Wang, Y. High-Rise Residential District Morphology Optimization for Enhancing the Green Space Cooling Effect. *Buildings* **2024**, *14*, 183. <https://doi.org/10.3390/buildings14010183>

Academic Editors: Baojie He and Haifeng Liao

Received: 22 November 2023

Revised: 21 December 2023

Accepted: 8 January 2024

Published: 11 January 2024



**Copyright:** © 2024 by the authors. Licensee MDPI, Basel, Switzerland. This article is an open access article distributed under the terms and conditions of the Creative Commons Attribution (CC BY) license (<https://creativecommons.org/licenses/by/4.0/>).

## 1. Introduction

Global urbanization continues to increase, and the urbanization level is expected to reach 68% in 2050 [1]. Large urban population concentrations have led to high-density urban development, especially in developing countries, which in turn has altered surface geometries and urban energy balances. This has introduced many problems to the urban climate environment, including global warming [2], the frequent occurrence of extreme weather [3], and air pollution. The urban heat island (UHI) effect is one of the most serious problems, jeopardizing the life and health of citizens [4], deteriorating the urban ecological environment, and increasing urban energy consumption [5]. As a result, many studies have been carried out on UHI effect mitigation.

### 1.1. Mitigation Effects of Urban Green Spaces on UHI

The causes of the UHI effect mainly include changes in subsurface characteristics and anthropogenic heat emission released by high energy consumption. Changes in subsurface characteristics include a decrease in natural vegetation, such as soil and water bodies, and an increase in impervious surfaces, such as concrete and tarmac [6]. To mitigate the UHI effect, large urban green spaces, as the most common blue and green infrastructure in cities, are able to optimize the urban climate by exerting a cool island effect via vegetation transpiration, which is considered to be an effective measure for cooling down a city sustainably [7–9]. Therefore, many studies have been conducted on the cool island effect of urban green spaces.

Research has shown that the cooling effect of green spaces is a complex phenomenon of multiple elements. On the one hand, the cooling effect is influenced by the characteristic of a green space itself, such as the size and shape of the green space and the composition of landscape elements [10–12]. Studies in this area started early and have produced

relatively mature research results. Among them, park size is the most important influencing factor [13]. The cooling intensity of an urban green space increases with its scale and decreases with distance [11]. The cooling range decreases with an increase in distance [14], ranging from tens of meters to more than 1 km [15,16]. In terms of time, it has been shown that the cooling effect of green spaces is strongest during summer nights [17].

On the other hand, the geometry of the built environment around a green space can further affect the cooling effect by influencing elements such as urban airflow and solar radiation. These include building density, floor area ratio, building height, building layout, and other morphological factors. As early as 2006, a study in Singapore using field measurement and ENVI-met simulation suggested the existence of the influence of building height and floor area ratio on the cooling effect of green space, but no quantitative results were developed [18]. A field measurement study of parks in Seoul, South Korea, demonstrated that building layout affects cold air dispersion [19]. Recently, a study of 36 green spaces in Xi'an using remote sensing showed that building densities of 0.25–0.3 and floor area ratios of 2.5–3 were more conducive to the diffusion of cooling effects in green spaces [20]. A study in Nanjing showed that a sparse high-rise building layout around a park was more favorable for the diffusion of cooling effects than a compact layout [21]. A study in Hangzhou analyzed the influence of building height, building intervals, and building orientation on the cooling effect of pedestrian levels in small urban parks. The building height has the greatest influence on the cooling intensity, which can reach 1.2 °C, and the building orientation has the greatest influence on the cooling distance, which can reach up to 100 m in the downwind direction [22]. The influence of the above built environment on the cooling effect of green spaces has produced extensive achievements, but they all focus on the height of pedestrians, and there is insufficient consideration of different heights in the vertical direction. In addition, there are more studies on related mechanisms and a lack of research on morphology optimization strategies.

### *1.2. Residential Block Spatial Morphology and Urban Climate*

The rapid advancement in urbanization in developing countries has brought about drastic changes in land cover and urban geometric features. Residential land use is the most common land use type in cities, which can account for 40% of a city [23]. As the basic unit of a city, the level of climate of residential blocks directly affects the thermal environment of an entire city. In China, high-rise residential blocks are the main type of high-rise buildings in Chinese cities. To mitigate the UHI effect, many studies have been conducted on the impact of residential planning and design factors on the urban climate.

Studies have analyzed the effects of the two-dimensional and three-dimensional indices of urban subsurface characteristics on the urban climate by means of field measurements and numerical simulations [23,24]. The two-dimensional morphology indices comprise different subsurface ratios, such as the greening cover ratio, impervious area ratio, and building density. Three-dimensional indices include the sky view factor, mean building height, floor area ratio, building orientation (BO), otherness [25], etc., where SVF mainly affects the received solar radiation. MBH and BO can affect solar radiation and wind speed and direction. Otherness can represent the overall height difference of a block, which can affect the solar radiation and wind environment. Most of these indicators are mandatory control indicators for urban planning [26], which have developed extensive achievements. In addition, the allocation of ground floor podiums is mandatory in Chinese settlements. Ground floor podiums affect the enclosure of the block, which in turn affects airflow and has an impact on the pedestrian-height microclimate. Therefore, it is still necessary to explore and propose refined settlement planning strategies for a certain refined morphology.

### *1.3. Motivation and Objective*

Xi'an is in the geographic center of China and located in a continental monsoon climate region. As of 2017, the city's area is 10,750 km<sup>2</sup> with a population of 12 million [27]. Xi'an



## 2. Materials and Methods

### 2.1. Selection of Study Area

This study takes Xi'an as the research object, and it has the typical characteristics of a first-tier city in a developing country. Established studies have shown that the green space that forms the cooling effect needs to have a greening rate of more than 40% and an area of more than 1.34 hm<sup>2</sup>. Based on this, XFLD was selected as a typical green space, which is located on the east side of the second ring road, where there is no influence of other large-scale green space cold sources near its upwind direction, and many high-rise residential areas are built on both sides of the adjacent green space. Furthermore, as shown in Figure 3a–c, in order to eliminate the uneven cooling effect at the two ends of the green space, we further chose the middle cross-section of this green space for field measurements and simulations.

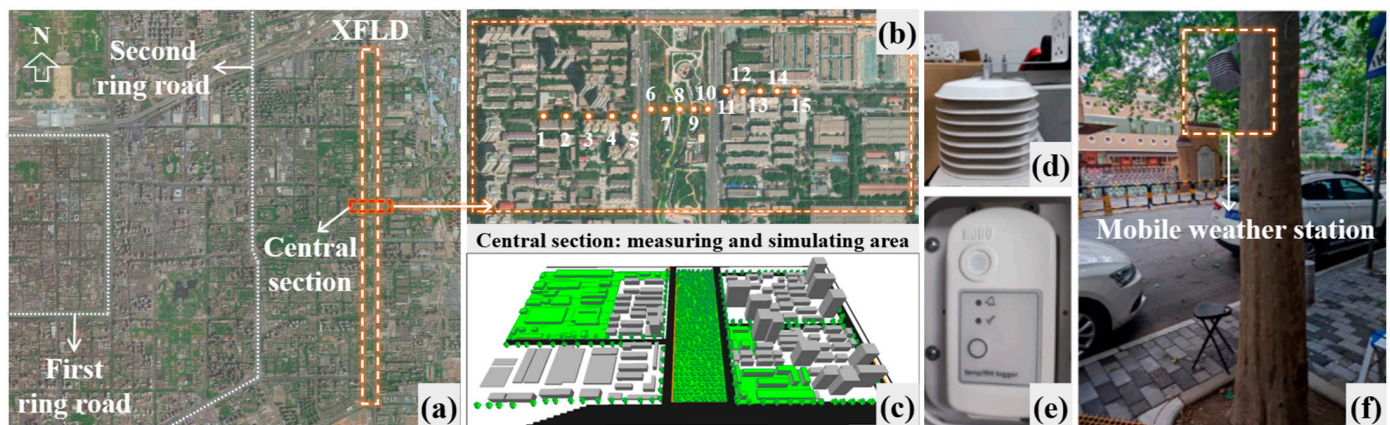


**Figure 3.** Field measurement and simulation-related information: (a) the location of the measurement section in XFLD; (b) distribution of the 15 measured points in selected central section of XFLD; (c) modeling of the measurement section in ENVI-met; (d) external louvered cover for mobile weather stations; (e) HOBO MX2301; (f) pedestrian-level view of the mobile weather stations installed under the tree canopy.

### 2.2. Evaluation of Simulation Software

This study uses ENVI-met 4.5 simulation software, which is one of the most widely used tools in the field of urban climate research. ENVI-met can analyze the impact of different urban built environment factors on urban climate [6,30].

To validate the software's performance, we measured the cross-section in the middle of XFLD on a clear and dry typical summer day from 18:00 on 23 August 2021 to 08:00 on 25 August 2021. This cross-section is located at the center of the cold island, and the residences on both sides contain slab-type and point-type towers for residential buildings and residential buildings of different heights, representing different subsurface characteristics of urban high-rise residences (Figure 3a). As shown in Figure 3e, we used a mobile weather station (brand and model: Onset HOBO MX2301) to measure the AT and relative humidity (RH). The AT and RH recording ranges were  $-40$ – $70$  °C and 0–100% RH, and the accuracies were  $\pm 0.2$  °C and  $\pm 2.5\%$ . To truly reflect the thermal environment at the pedestrian level, as shown in Figure 3f, the measurement height was set at 2 m above the ground under the tree canopy. All sensors had louvered covers to ensure ventilation and prevent solar radiation (Figure 3d). A total of 15 measurement points were arranged for the field measurement (Figure 3b). When arranging the measurement points, we chose to extend the green space at the center at both sides for an equidistant distribution of points.

Based on Google Maps and field investigations, we constructed the ENVI-met model (Figure 3c). The simulation time was consistent with the measured time, and the average AT and RH of the 15 measurement point data were used as meteorological input parameters. The wind speed (WS) and direction were adopted from the meteorological data of the

weather station, in which the WS was 1.5 m/s and the wind direction was northeast. The rest of the meteorological parameters are adopted from the EnergyPlus Weather data of the day. Figure 4 demonstrates the measured and simulated hour-by-hour AT, with an overall  $R^2$  value of 0.912, a root-mean-square error (RMSE) of 1.906 for the AT, and an RMSE value of 0.485 for RH, which proves that the ENVI-met simulation results and measured values are extremely correlated and have high accuracy in microclimate simulations.

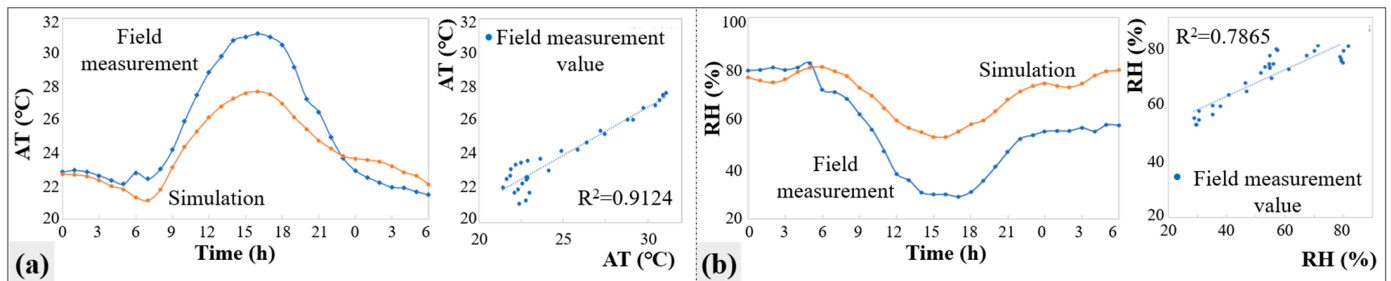


Figure 4. Validation of measured and simulated data: (a) AT; (b) RH.

### 2.3. Selection of Morphological Indices

To explore the factors of urban morphology that may cause differences in the spread of cooling effects, based on the simulation results of the real scenario in Section 2.2, we extracted the simulation results with the highest AT and the largest AT difference at each point (15:00). At the same time, to avoid the influence of the model boundary value, we chose the downwind direction of the southwest side of a green area near the central green area for the analysis. Through comparison, it was found that particularly significant ATs and wind variations were found in the three groups of areas, with significant differences in BO, the degree of enclosure of podiums, and building heights, with close building densities and development intensities in their domains. Based on this, as shown in Figure 5a, we identified three indices: BO, podium ration (PR), and otherness.

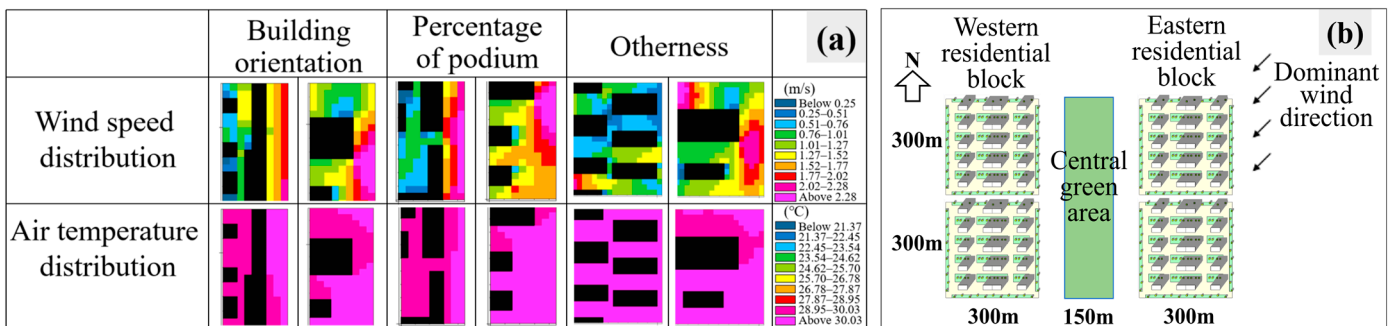


Figure 5. (a) Areas with significant differences in thermal environments in the realistic model; (b) schematic diagram of the ideal models.

### 2.4. Modeling of Typical Residential Blocks

#### 2.4.1. Morphological Characterization Investigation of Existing Residential Blocks

We extracted point-of-interest data from Baidu Map (<https://lbsyun.baidu.com/> (accessed on 25 September 2021)) for settlements built after 2010 and obtained a total of 578 high-rise blocks. Figure 6 illustrates their floor area ratio and building size parameters. The results show that 48% of the residential blocks have site areas between 4 and 16.2 ha. The average length of the blocks is 280 m; the average width is 270 m. Moreover, 62.3% of the blocks have floor area ratios concentrated within 2.8–5.1 and greening ratios concentrated within 30–40%. The length of high-rise buildings is mainly 50 m–70 m; the width of buildings is mainly 15 m–25 m; and 61% of the buildings are oriented mainly in the north–south direction. Among them, 42% of the residential blocks are equipped with

commercial podiums, and 73% of the commercial podiums have a height of three floors. Based on this, 300 m × 300 m is chosen as the side length of a typical residential block, and 30 m × 15 m is chosen as one unit of a slab unit, which is the same as in a similar study [12]. The highest building is 27 stories, and 25 stories is commonly used. The floor area ratio of the residential area is 2.5, with a building density of 11% and a greening rate of 35%.

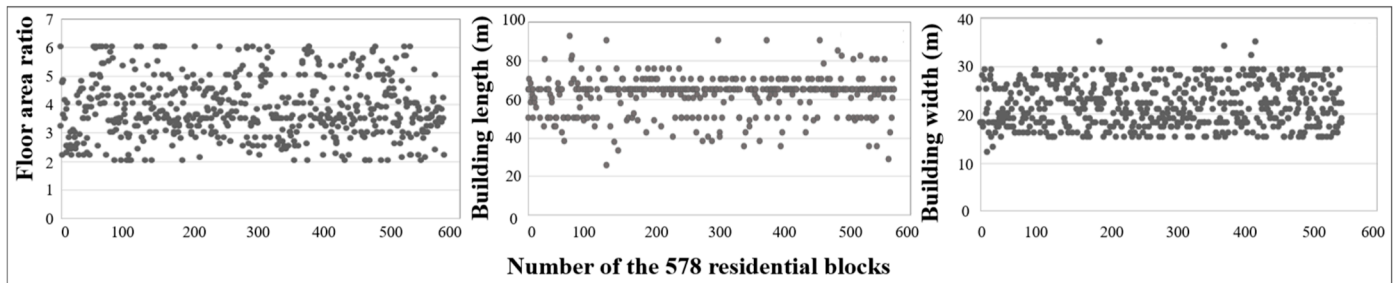


Figure 6. Characteristics of residential buildings in Xi’an.

### 2.4.2. Construction of Three Ideal Model Groups

To analyze the relationship between the green space and the residential blocks, the residential blocks are arranged in the upstream and downstream wind direction of the green space. The dominant wind direction in Xi’an is northeast in summer, as shown in Figure 5b, so the residential blocks are arranged along the east and west sides of the green space. Based on the common BO, PR, and building height layout patterns in Chinese settlements [31], a total of 16 simplified ideal models are set up for the three morphology indices. Figure 7 shows a schematic diagram of the 16 ideal models, taking the residential block in the northwest corner in Figure 5b as an example, with the green space to the east of it. Table 1 quantifies the differences between the 16 models.

Building orientation (BO)	perpendicular		parallel					
Buildings are perpendicular or parallel to the green space along the green space side.								
Podium ratio (PR)	0      30%      80%      100%				perpendicular			
The podium ratio on the perimeter of the block, which reflects the degree of enclosure of the block.					parallel			
Otherness	0      0.16      0.32			Perpendicular	0      0.16      0.32			Parallel
Ratio of the standard deviation of the height of all buildings in the block to the average height. It is calculated as follows: $O = \sigma / H$ where O means otherness, $\sigma$ means the standard deviation of the height of all buildings in the block, H means the average height of all buildings in the block.				<b>Otherness pattern 1 (OP1): Sequencing</b>				<b>Otherness pattern 2 (OP2): Center symmetry</b>

Figure 7. Three ideal model groups (16 models in total).

**Table 1.** Morphological parameters of three groups of ideal models (corresponding to three morphological indices).

Indices	Group No.	Model No.	Value of BO	Value of PR	Otherness Pattern	Value of Otherness
Building orientation along the greenbelt side (BO)	G1	1	perpendicular	null	null	null
		5		null		null
Podium ratio along the greenbelt side (PR)	G2	1	perpendicular	0%	null	null
		2		30%		null
		3		80%		null
		4		100%		null
	G3	5	parallel	0%	null	null
		6		30%		null
		7		80%		null
		8		100%		null
Otherness	G4	1	perpendicular	null	pattern 1 (OP1) *	0
		9		null		0.16
		10		null		0.32
	G5	5	parallel	null	pattern 1 (OP1) *	0
		11		null		0.16
		12		null		0.32
	G6	1	perpendicular	null	pattern 2 (OP2) *	0
		13		null		0.16
	G7	14	parallel	null	pattern 2 (OP2) *	0.32
		5		null		0
		15		null		0.16
			16		null	

Note: OP1 \* is the sequential increase in building height starting with the building along the green side, which is the lowest building. OP2 \* is a symmetrical change in building height from the center building of the block in all directions from high to low, with the center building being the tallest.

- For BO, two models were set up, one perpendicular and one parallel to the green space.
- For PR, four different PR values were set to represent different degrees of openness.
- For otherness, two otherness patterns were set up; otherness pattern 1 (OP1) is the sequential increase in building height starting with the building along the green side, which is the lowest building. Otherness pattern 2 (OP2) is the symmetrical change in building height from the center building of the block in all directions from high to low, with the center building being the tallest.

### 2.5. Modeling Settings

We set up 16 models in ENVI-met. A grid of 5 m × 5 m × 3 m was set up, totaling 219 × 108 × 40 grids. The hour-by-hour AT and RH data on 24 August after averaging the measured data with the realistic simulation data were used as the input data. The wind speed (WS) and direction were adopted from the meteorological data of the weather station, in which the WS was 1.5 m/s and the wind direction was northeast, which is consistent with a typical summer day in Xi'an according to the Chinese residential design standards [26]. The rest of the meteorological parameters were adopted from the EnergyPlus Weather data of the day. The geographic location of the study area was established as Xi'an City. The time pace of the simulation was 10 s, and the simulation start time was 18:00 on 23 August 2021, with a simulation duration of 36 h.

### 3. Results

#### 3.1. Characterization of the Cold Island Effect in Typical Green Spaces

The cooling effect of XFLD is analyzed by combining the field measurements and the simulation results of the real scenario. The field measurements show that the cooling effect is most significant at 23:00. Figure 8a demonstrates the AT of the section at 23:00, and the AT of the central green space is significantly lower than that of the residential blocks on both sides, with a maximum AT difference of up to 2 °C. The average AT at 23:00 at the five measurement points in the central green space was 1.5 °C lower than that in the west and 1 °C lower than that in the east. This is due to the fact that the building heights on either side of the green space are significantly higher than those in the green space itself, thus creating a large shaded area inside the block during the daytime, avoiding direct solar radiation. In contrast, the interior of the green space absorbed all the solar radiation during the daytime, so the AT at the pedestrian level was higher during the daytime and did not reflect a significant cooling effect. In the absence of solar shortwave radiation at night, transpiration from the green space vegetation lowered the AT, while the high-rise buildings inside the blocks on both sides began to release the heat absorbed during the day through longwave radiation, resulting in higher ATs in the residential blocks on both sides.

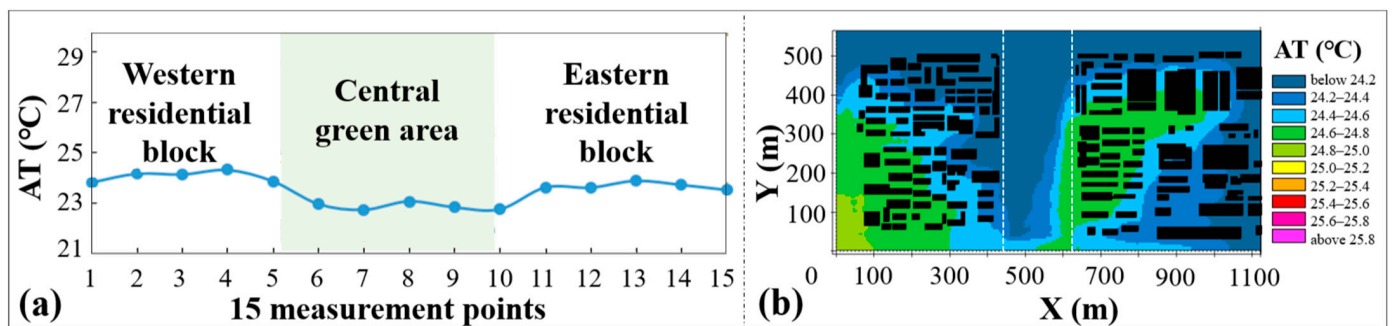


**Figure 8.** (a) Distribution of AT at each measurement point at 23:00 in the section; (b) AT simulation results at 23:00 in the realistic model in the section.

Figure 8b shows the AT simulation results at 23:00, where the greenfield AT is significantly lower and exerts a significant cooling diffusion effect downwind. Note that the green space exerts a significant cooling diffusion effect towards the middle of the western parcel, with a downwind diffusion distance of up to 250 m to the west due to the fact that the middle of the western parcel is significantly more open without a podium. Therefore, the wind produces a more significant cooling effect spread. The cooling effect is the strongest at 150 m, with the cooling effect decreasing by 0.2 °C from 150 m to 250 m. The AT is significantly higher in the southwest corner of the western blocks, which may be attributed to the higher building height there. The high development intensity leads to higher anthropogenic heat emission, which results in a higher average AT in the west than in the east.

#### 3.2. Influence of High-Rise Residential Block Morphology on the Cooling Effect of Green Space

As shown in Figure 9a, the model is divided into 12 equal sections along the east–west direction (transverse) based on the wind direction—with each section spaced 50 m apart and four sections in each of the three east, center, and west regions—to compare the thermal environment of the green space and upwind and downwind residential blocks. Based on the simulation results, the AT, RH, and mean radiant temperature (MRT) for the different ideal models at the pedestrian level and the WS and AT distribution characteristics for different longitudinal heights of 10 m, 30 m, 50 m, and 80 m are plotted. The effects of the green-side BO, PR, and otherness on the cooling of the green island are analyzed.

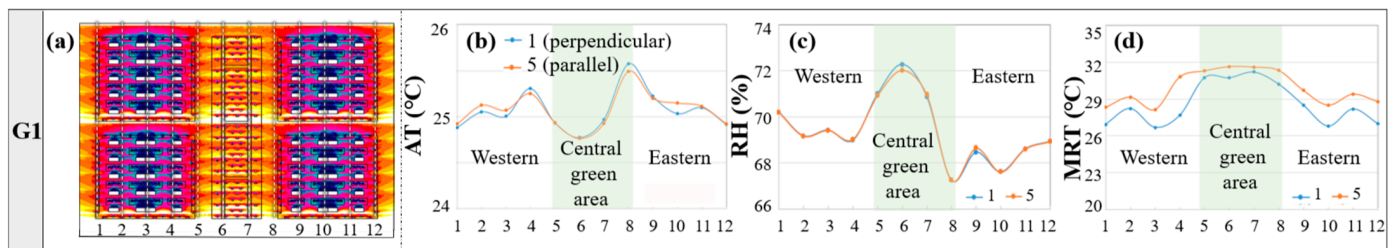


**Figure 9.** (a) Daylight analysis and schematic diagram of 12 sections for model 1; average daily AT, RH, and MRT distribution of 12 sections at the pedestrian level in model G1: (b) AT; (c) RH; (d) MRT.

### 3.2.1. Influence of BO along the Green Side on Cooling Effects

#### 1. At the pedestrian level

There is one group of models (G1) for BO, as shown in Figure 7. Model 1 is laid out perpendicularly to the greenbelt along the greenbelt side of the building, and model 5 is laid out in a parallel manner. At the pedestrian level, Figure 9b–d show the AT, RH, and MRT at a pedestrian level of 1.5 m.

- AT

Figure 9b shows the average AT for each cross-section of Models 1 and 5, where the upwind eastern block of both Models 1 and 5 has higher AT than the downwind western block, suggesting that the green space embodies a cooling effect downwind. In addition, the AT is lower for the four sections of model 1, which is 0.1 °C lower than that of Model 5.

- RH

Figure 9c show the comparison the RH of the east and west blocks, with a significant humidification effect of 1.1% in the downwind direction of the green space.

- MRT

The MRT of model 1 is also lower, but the difference between the east and west plots is not significant, suggesting that the cooling effect does not have much influence on the MRT.

Overall, the buildings along the green space that are laid out perpendicularly (model 1) at the pedestrian level are more conducive to the diffusion of the cooling effect of the green space and have a lower MRT.

#### 2. At different heights in the vertical direction

- WS

At different heights in the vertical direction, changing the BO has a significant effect on the WS and AT below 50 m and no significant effect at 80 m.

Figure 10a illustrates the average daily WS at 10 m, 30 m, 50 m, and 80 m. Overall, the difference in WS between the different sections decreases with height. In addition, Figure 9a shows the section 8 at 10 m is located upwind of the greenbelt, where the combined effect of urban winds and the tree canopy will create a larger WS, whereas WSs are weakened within the greenbelt due to tree foliage, but not at heights above the tree canopy.

- AT

Figure 10b illustrates the daily average AT for each section at different heights. Overall, the vertical layout has a lower AT up to 50 m, with no difference between the two BOs at 80 m. Anomalous fluctuations were observed in sections 3 and 10 at heights of 10 m, 30 m, and 50 m. Combined with the insolation analysis in Figure 9a, a 1.28 °C variation is formed due to the proximity to the building wall, which is different from the open environment of the other sections. In addition, the AT is also lower downwind of the buildings along the street when they are perpendicular to the greenbelt, contributing to the greenbelt's cooling effect in the settlement, and the overall AT is also lower in the west, center, and east.

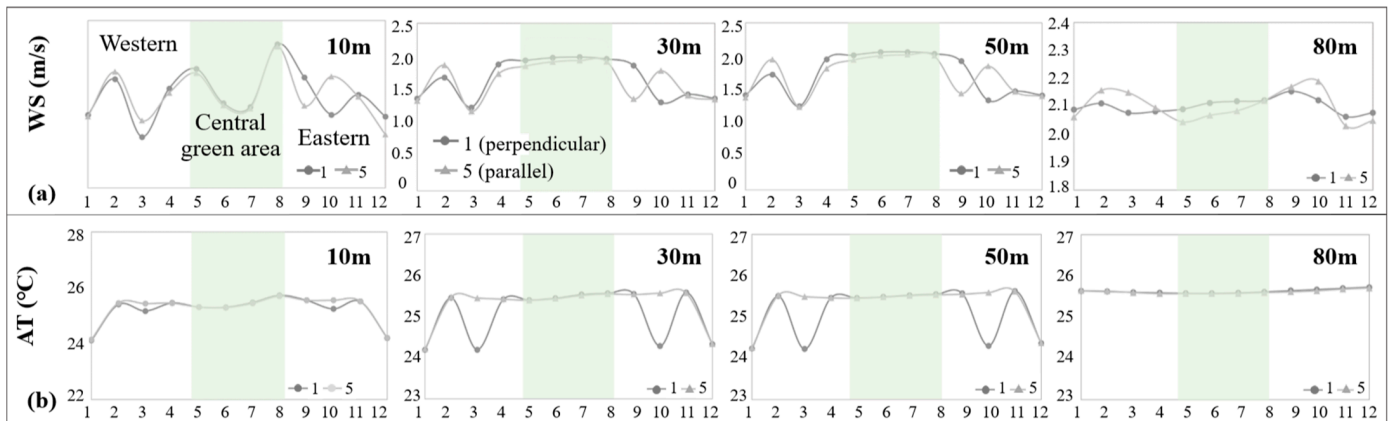


**Figure 10.** Distribution of daily average WS and AT for 12 sections at 10 m, 30 m, 50 m, and 80 m heights for model G1: (a) WS; (b) AT.

### 3.2.2. Influence of PR along the Green Side on Cooling Effects

#### 1. At the pedestrian level

There are two groups of models (G2 and G3) for the PR along the greenbelt side. In terms of pedestrian levels, Figure 11 shows the AT, RH, and MRT for each section of G2 and G3.

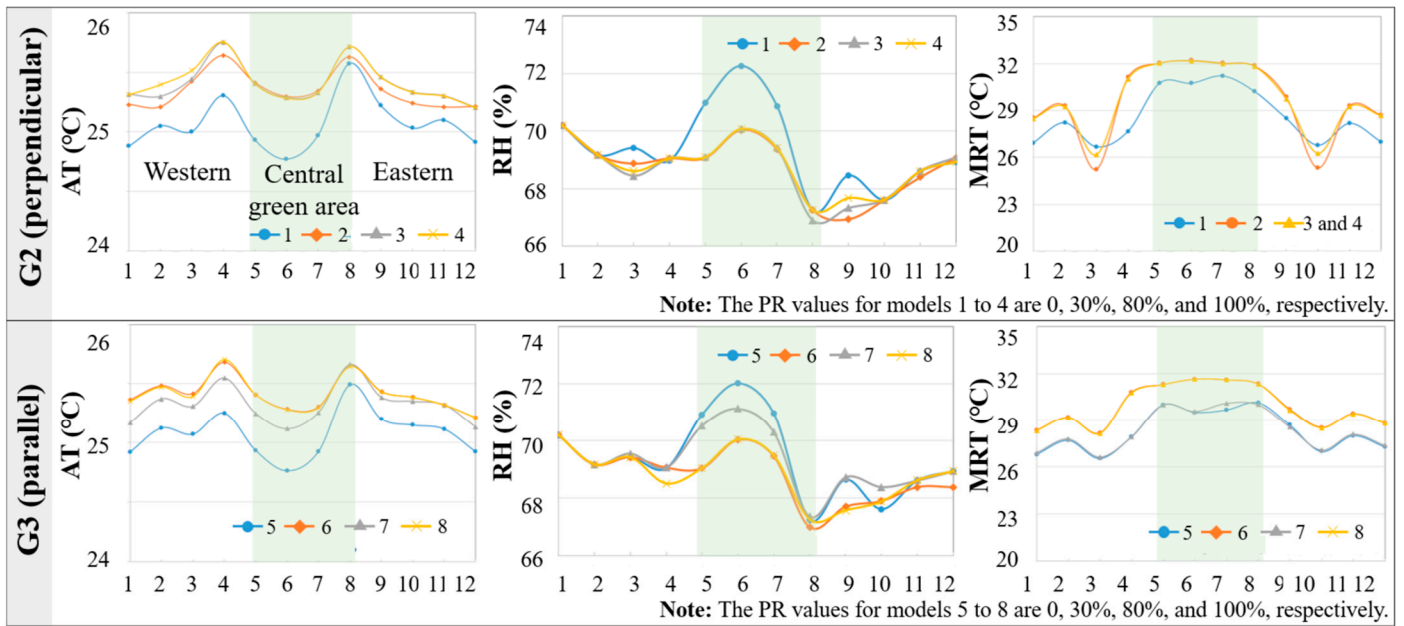


**Figure 11.** Distribution of daily average AT, RH, and MRT for 12 sections at the pedestrian level for different PR models G2 and G3.

- Perpendicular

G2 shows the results of different PRs when buildings are laid out perpendicular to the greenbelt. Model 1, with a PR of 0, performs the best with the lowest AT and MRT and the highest RH, and the AT in the downwind area is lower than that in the upwind area, which means the greenbelt in the middle has a significant cooling effect. At 30%, 80%, and 100% PRs, the thermal environment is not as good as it could be at 0 and does not reflect a cooling effect.

- Parallel

When the buildings along the greenbelt side are parallel to the greenbelt in G3, model 5, with a PR of 0, performs the best, and the entire area exhibits the lowest AT and MRT and the highest RH. Meanwhile, the western AT is lower than the central one, reflecting the diffusion of the cooling effect. Model 7, with an 80% PR, also reflects the cooling effect, while the performance of the MRT is close to that of model 1. The models with 30% and 100% PRs perform worst. This may be because at an 80% PR, the openings between the podiums form an “isthmus effect”, which increases the WS and results in a circulation of wind between the plots, further resulting in the cooling of the plots.

This shows that when there is no podium on the windward side, the thermal environment of the blocks at the pedestrian level will be better than when there is a podium. In addition, when the buildings along the street are parallel to the green space and the PR is 80%, there will also be a good cooling effect.

2. At different heights in the vertical

At different heights relative to the longitudinal direction, Figure 12 demonstrates the average WS and AT throughout the day for each 10 m, 30 m, 50 m, and 80 m section for models G2 and G3. The results show that a different PR can have a significant effect on the WS at a height of 10 m and the AT at a height of below 80 m.

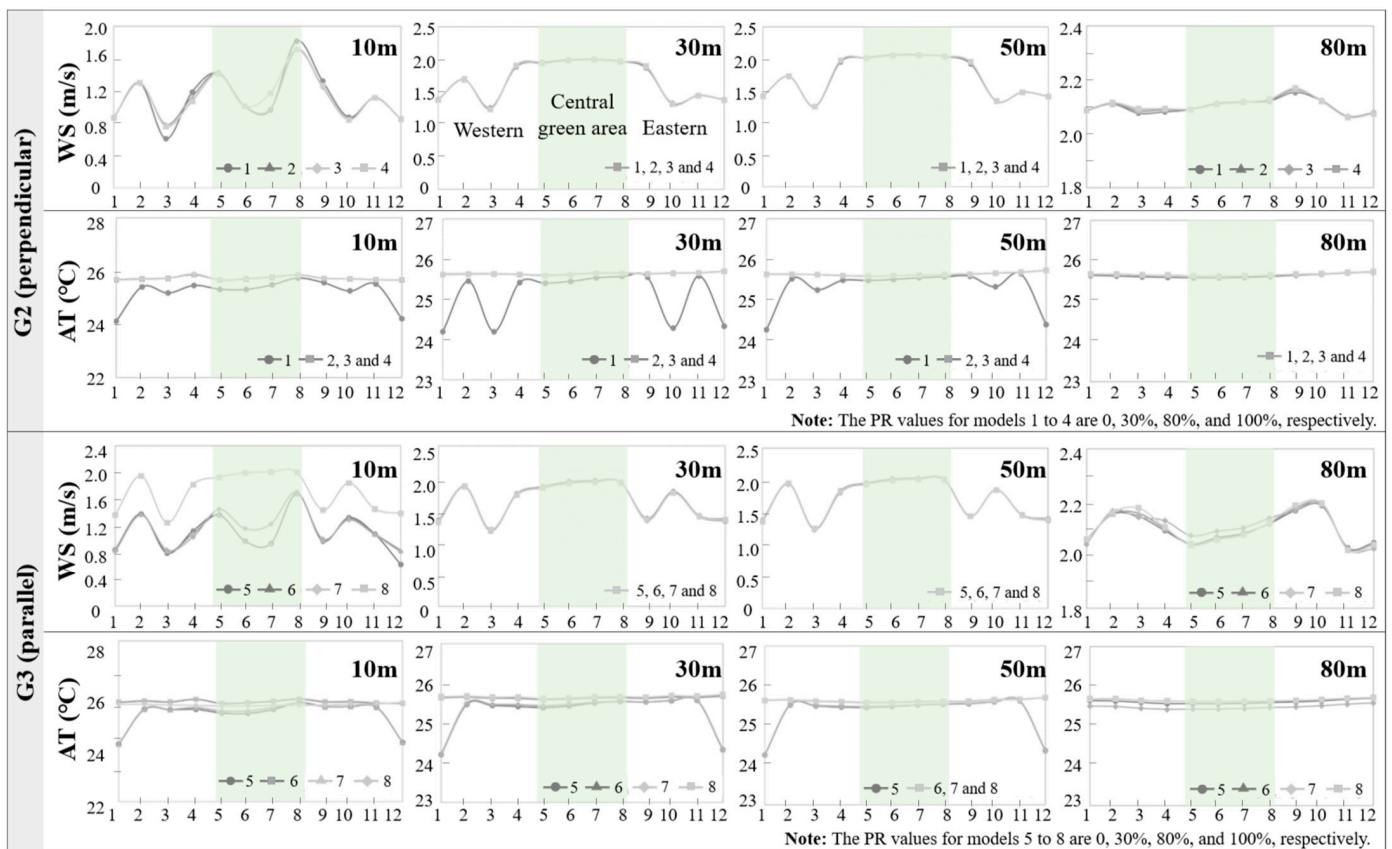


**Figure 12.** Distribution of daily average WS and AT for 12 sections at 10 m, 30 m, 50 m, and 80 m heights for PR models G2 and G3.

- Perpendicular

The results of G2 show that when the buildings along the side of the greenbelt are perpendicular and the PR is 0, the WS and AT at 10 m perform best, and a better low-temperature linkage can be formed between the center green space and downwind settlements, which is consistent with the results for the 1.5 m pedestrian level. Moreover, the

30 m and 50 m models also have significantly lower ATs than the other models. Model 4 shows that when the PR is 100%, the average WS in the middle green space at a 10 m height is the lowest, which is not conducive to the diffusion of cooling effects. Therefore, when considering the thermal environment at a 10 m height, the case where the buildings along the green side are perpendicular and the PR is 100% is not recommended.

- Parallel

When the buildings along the green side are parallel, the WS at 10 m with a 100% PR is the highest, which is 1.17 m/s higher than the WS without a podium. Above 10 m, different PRs have little effect on the WS. In addition, the models with 0 and 80% PRs have the lowest ATs at 10 m and 30 m, while those with 50% and 100% PRs perform the worst.

Taken together, increasing the PR has a significantly detrimental effect on the cooling effect of the greenbelt below 50 m by altering the windward area of the ground floor. Arranging podiums when the buildings along the green side are perpendicular is not recommended. When the buildings along the street are parallel to the direction of the green space and the PR is 80%, this will produce similar optimization effects to the case with no podiums, which is worth using as a reference in designs.

### 3.2.3. Influence of Otherness on Cooling Effect

There were four groups of models (G4–G7) with different values of otherness, with pattern 1 (OP1) for G4 and G5 and pattern 2 (OP2) for G6 and G7 (Figure 7).

#### 1. At the pedestrian level

In terms of pedestrian levels, Figure 13 shows the AT, RH, and MRT for each section of the four groups.

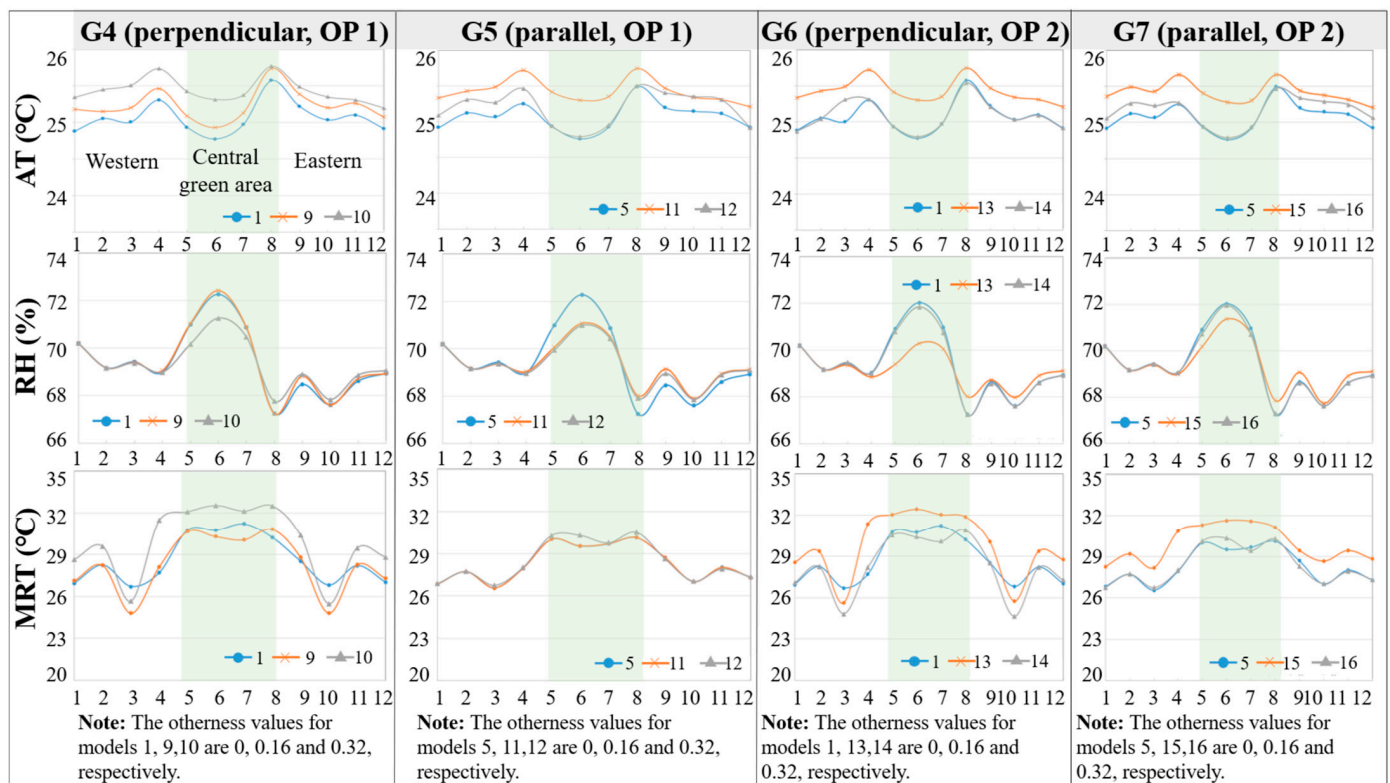


**Figure 13.** Distribution of daily average AT, RH, and MRT for 12 sections at the pedestrian level for different otherness models G4–G7.

- OP1

When the otherness is OP1 and the buildings are laid out perpendicularly to the green space along the green-space side, there is a cooling effect when the AT in the west is lower than the AT in the east at otherness values of 0 and 0.16. Meanwhile, this model has a lower AT and MRT and a higher RH. The higher the otherness, the higher the AT of the model. When the otherness value is 0.32, this model has the highest AT and MRT, and the central green space does not reflect a cooling effect. Therefore, using 0 or 0.16 for the perpendicular layout is recommended, and 0.32 should be avoided. When the parallel layout of buildings along the side of the green space is used, the AT, RH, and MRT are the best when the otherness is 0; the otherness in the west is lower than that on the east side, and there is a significant cooling effect. There is no cooling effect at otherness values of 0.16 and 0.32, and the model has the highest AT at 0.16. Therefore, it is best to use 0 for the parallel case, and 0.16 and 0.32 are not recommended.

- OP2

When the otherness is OP2, regardless of whether the perpendicular or parallel case is used, an otherness value of 0.16 performs the worst, with the highest AT and MRT and the lowest RH. Also, there is no cooling effect. A cooling effect exists both perpendicularly and parallelly at otherness values of 0 and 0.32. Therefore, when otherness adopts the OP1 layout and the perpendicular layout of the buildings along the side of the green space is used, an otherness value of 0 or 0.16 is recommended, and 0.32 should be avoided; 0 is the best in the parallel case. In the OP2 layout, the otherness value should be taken as 0 or 0.32, and 0.16 is not recommended regardless of whether the buildings along the side of the green space are perpendicular or parallel.

## 2. At different heights in the vertical direction

With respect to different height, Figures 14 and 15 show the daily average WS and AT for each 10 m, 30 m, 50 m, and 80 m section for the four groups, G4–G7. Changing the otherness has the most significant effect on the WS at 80 m, and the fluctuation of the WS between the sections is most obvious at an otherness of 0.32, with a maximum difference of 0.49 m/s in G5. The difference is not significant below 50 m. The opposite is true for the AT, where changing the otherness has no significant effect on the AT at 80 m, and the AT at 50 m and below has a significant effect. For the WS, when the otherness value is 0.32, the WS at a 30 m–80 m height is significantly higher than that of the other models, regardless of the parallel or perpendicular case and regardless of OP1 or OP2, which is conducive to the diffusion of cooling effects.

- OP1

When the otherness is OP1 and the perpendicular layout is used, otherness values of 0 or 0.16 reflect lower ATs and cooling effects at 10 m, 30 m, and 50 m, with a maximum cooling of down to 1.83 °C. There was no significant effect with respect to a change in otherness on different heights relative to the longitudinal direction in the parallel case.

- OP2

When the otherness was OP2, regardless of the perpendicular or parallel layout, the 10 m height of the model with an otherness value of 0 or 0.32 embodied a lower AT and significant cooling effects. The otherness value of 0.16 had the worst effect. At a 30–80 m height, 0 and 0.32 embodied lower ATs, but the cold diffusion effect was not significant.

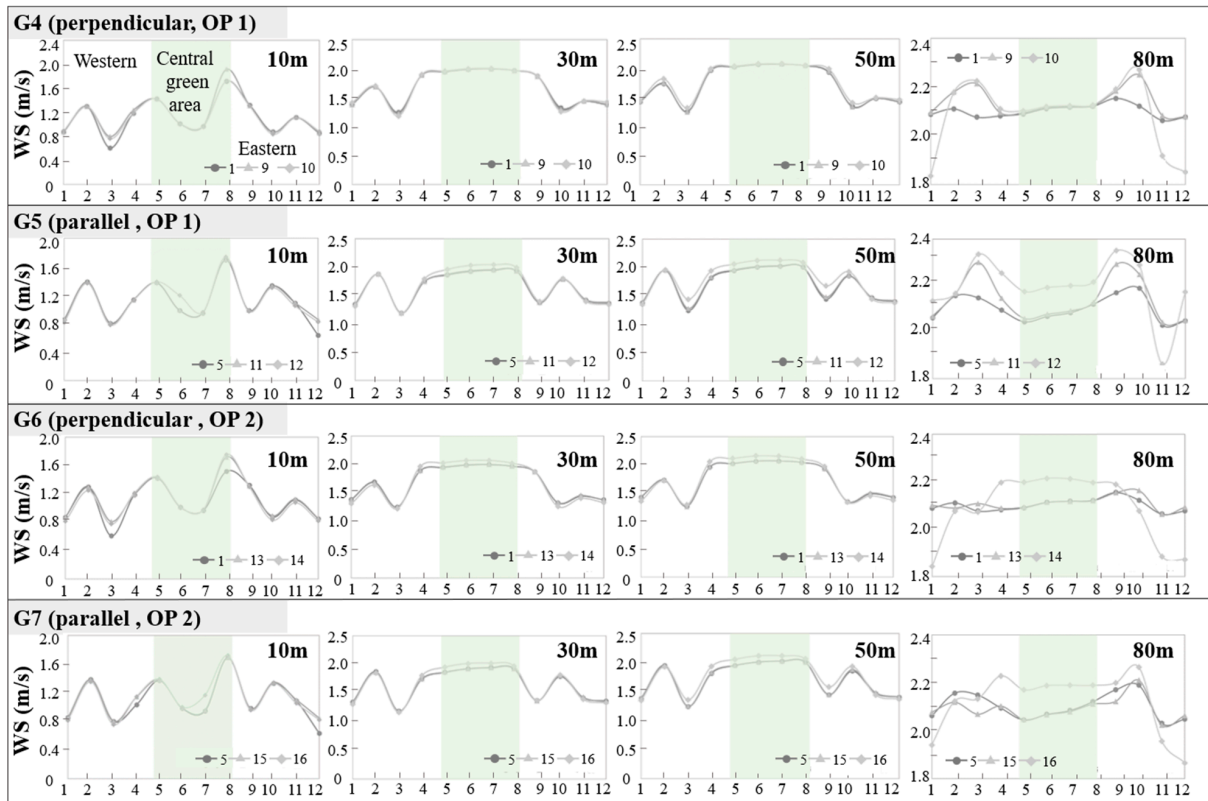


Figure 14. Distribution of daily average WS for 12 sections at 10 m, 30 m, 50 m, and 80 m heights for otherness models G4–G7.

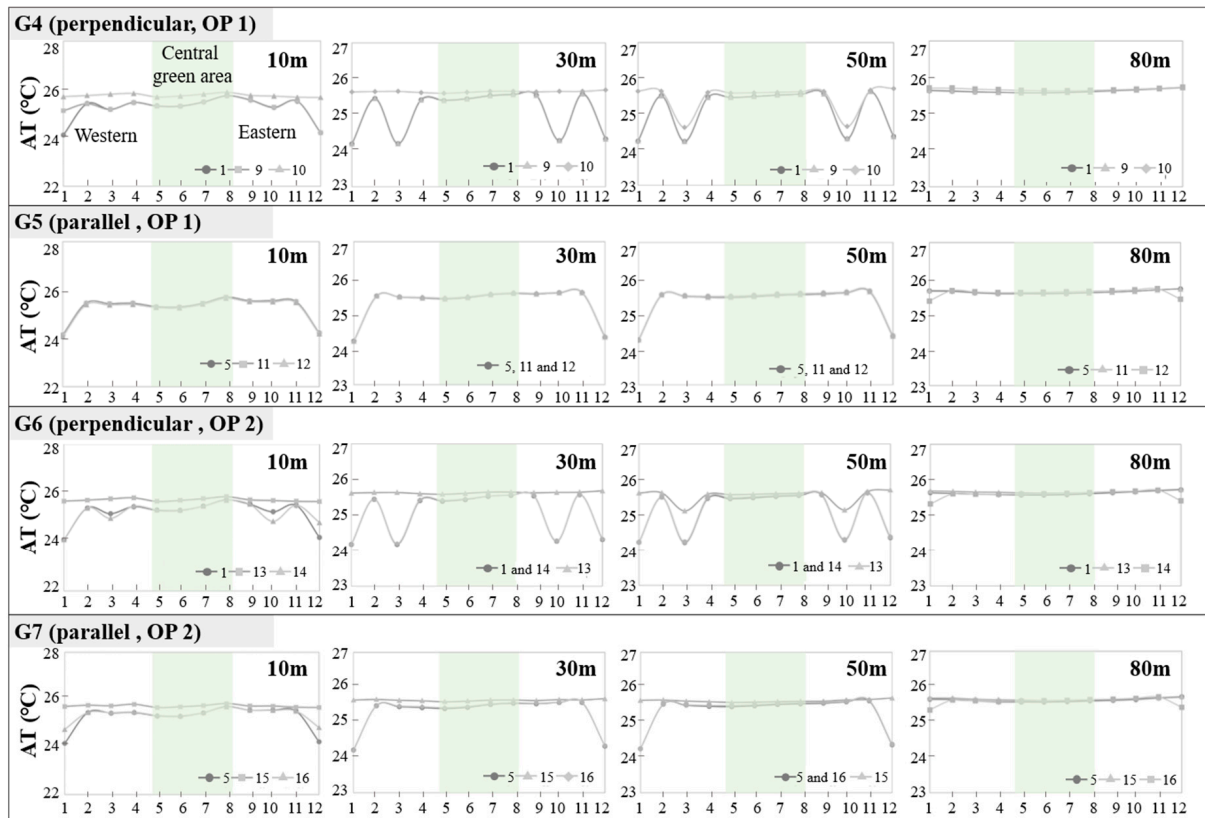


Figure 15. Distribution of daily average AT for 12 sections at 10 m, 30 m, 50 m, and 80 m heights for otherness models G4–G7.

#### 4. Discussion

This study verified the spatial and temporal characteristics of the cooling effect of large urban green spaces and the influence of the surrounding building morphology on the cooling effect through field measurements and simulations. The results show that in terms of the intensity of the cooling effect, the cooling intensity can reach 2 °C; spatially, the cooling distance can spread up to 250 m; and temporally, the cooling effect is most significant at night. This is consistent with many similar studies. Research in Chongqing, a hot and humid city in China, showed that the intensity of a green space cool island of 4.5 ha can reach 2 °C [32]. A study on 262 urban green spaces in Bangalore, India, a city in a developing country, showed that the cooling effect of green spaces during daytime in summer averaged 2.23 °C, with median and mean cooling distances of 270 m and 347 m [14]. It has also been shown that the cooling range of a park is roughly equal to the width of the park [33]. A study in Changchun, China, showed that green spaces have the highest cooling intensity at night in summer [17]. A field measurement study in Japan showed that the cooling effect of large green spaces during summer nights can reach 200 m–300 m in urban areas, and the cooling distance of this study is consistent with our study. However, this study found that the cooling effect during the daytime is stronger than at night, the maximum cooling intensity during the daytime can be up to 1.9 °C, and the cooling distance can be more than 300 m [34]. This is because the green space in the Japanese study area is surrounded by two-story residential houses, which differs from the built-up environment with a high density in the urban area of China where our study is located. Therefore, multiple factors, such as development intensity and the building layout around the green space, can significantly influence the difference in the green space cooling effect, and high-density, high-rise buildings and low-density, low-rise buildings may cause opposite results. Therefore, the influence of finer urban morphology on the cooling effect of green spaces in the future needs to be further explored. There are some limitations to this study, which only discussed the cooling effect in summer and lacked a winter-related analysis, and subsequent studies should comprehensively analyze the results of winter and summer seasons.

#### 5. Conclusions

This study focuses on high-rise residential blocks around green spaces and simulates their thermal environment at the internal pedestrian level and at different heights relative to the longitudinal direction. Based on the comparison results of BO, PR, and otherness, optimization strategies are proposed. When only the BO along the green side is changed, it is recommended that the BO is set to the perpendicular configuration, which is more conducive to the diffusion of the cooling effect in the central green area and produces a lower MRT at the pedestrian level and a lower AT below 50 m. When only changing the PR, residential blocks without podiums will create a more optimal climate. However, podiums are usually a mandatory feature in Chinese residential design. Therefore, we recommend using a 30% PR for the perpendicular layout of buildings along the green side with a lower pedestrian-level AT and MRT, which is better than 80% and 100% PRs. In parallel, an 80% PR is recommended in order to have a cooling effect at the pedestrian level of up to 1.83 °C while simultaneously having a lower AT at 10 m and 30 m of up to 0.83 °C. For block otherness, when the otherness is PO1 and the perpendicular building layout along the green side is used, otherness values of 0 and 0.16 are recommended, but not 0.32; when a parallel layout is used, an otherness value of 0 is recommended. When the otherness is PO2, values of 0 or 0.32 are recommended, which exhibit better AT diffusion and cooling effects at the pedestrian level and different longitudinal heights; 0.16 is not recommended.

Overall, this study draws the following conclusions: (1) The cooling effect of the green space is the strongest up to 150 m; the cooling effect decreases from 150 m to 250 m; and the cooling amplitude can be up to 2 °C along the downwind direction. (2) The design strategy of high-rise residential blocks around the green space to maximize the cooling effect is proposed based on three morphology indices, namely, BO, PR, and otherness,

which provides a basis and guideline for planners and architects to formulate design schemes of climate-adapted residential areas.

**Author Contributions:** Conceptualization, F.S. and Y.W.; methodology, F.S.; formal analysis, Y.C. and W.Y.; investigation, F.S. and Y.W.; writing—review and editing, F.S., Y.C. and Y.W.; visualization, Y.C.; supervision, Y.W.; funding acquisition, Y.W. All authors have read and agreed to the published version of the manuscript.

**Funding:** This research was funded by the National Natural Science Foundation of China (grant number 52078416), Fundamental Research Funds for the Central Universities (grant number xzy022022042), and the Buildings 2023 Travel Award.

**Data Availability Statement:** Data are contained within the article.

**Conflicts of Interest:** The authors declare no conflicts of interest.

## References

1. DAES. *World Urbanization Prospects 2018: Highlights*; United Nations: New York, NY, USA, 2019.
2. Wu, F.; Geng, Y.; Tian, X.; Zhong, S.; Wu, W.; Yu, S.; Xiao, S. Responding climate change: A bibliometric review on urban environmental governance. *J. Clean. Prod.* **2018**, *204*, 344–354. [\[CrossRef\]](#)
3. Soon, W.W.-H.; Connolly, R.; Connolly, M.; O'Neill, P.; Zheng, J.; Ge, Q.; Hao, Z.; Yan, H. Comparing the current and early 20th century warm periods in China. *Earth-Sci. Rev.* **2018**, *185*, 80–101. [\[CrossRef\]](#)
4. Puvvula, J.; Abadi, A.M.; Conlon, K.C.; Rennie, J.J.; Herring, S.C.; Thie, L.; Rudolph, M.J.; Owen, R.; Bell, J.E. Estimating the Burden of Heat-Related Illness Morbidity Attributable to Anthropogenic Climate Change in North Carolina. *Geohealth* **2022**, *6*, e2022GH000636. [\[CrossRef\]](#)
5. Santamouris, M.; Cartalis, C.; Synnefa, A.; Kolokotsa, D. On the impact of urban heat island and global warming on the power demand and electricity consumption of buildings—A review. *Energy Build.* **2015**, *98*, 119–124. [\[CrossRef\]](#)
6. Chen, Y.; Wang, Y.P.; Zhou, D. Knowledge Map of Urban Morphology and Thermal Comfort: A Bibliometric Analysis Based on CiteSpace. *Buildings* **2021**, *11*, 427. [\[CrossRef\]](#)
7. Jamei, E.; Rajagopalan, P.; Seyedmahmoudian, M.; Jamei, Y. Review on the impact of urban geometry and pedestrian level greening on outdoor thermal comfort. *Renew. Sustain. Energy Rev.* **2016**, *54*, 1002–1017. [\[CrossRef\]](#)
8. Oliveira, S.; Andrade, H.; Vaz, T. The cooling effect of green spaces as a contribution to the mitigation of urban heat: A case study in Lisbon. *Build. Environ.* **2011**, *46*, 2186–2194. [\[CrossRef\]](#)
9. Shi, M.; Wang, Y.; Lv, H.; Jia, W. Climate gentrification along with parks' cooling performance in one of China's tropical industrial cities. *Sci. Total Environ.* **2023**, *892*, 164603. [\[CrossRef\]](#)
10. Xue, S.; Chao, X.; Wang, K.; Wang, J.; Xu, J.; Liu, M.; Ma, Y. Impact of Canopy Coverage and Morphological Characteristics of Trees in Urban Park on Summer Thermal Comfort Based on Orthogonal Experiment Design: A Case Study of Lvyin Park in Zhengzhou, China. *Forests* **2023**, *14*, 2098. [\[CrossRef\]](#)
11. Shi, M.; Chen, M.; Jia, W.; Du, C.; Wang, Y. Cooling effect and cooling accessibility of urban parks during hot summers in China's largest sustainability experiment. *Sustain. Cities Soc.* **2023**, *93*, 104519. [\[CrossRef\]](#)
12. Gao, N.; Zhang, H.; Wang, P.; Ning, L.; Wong, N.H.; Yu, H.; Ke, Z. Research on Microclimate-Suitable Spatial Patterns of Waterfront Settlements in Summer: A Case Study of the Nan Lake Area in Wuhan, China. *Sustainability* **2023**, *15*, 15687. [\[CrossRef\]](#)
13. Yu, Z.; Yang, G.; Zuo, S.; Jørgensen, G.; Koga, M.; Vejre, H. Critical review on the cooling effect of urban blue-green space: A threshold-size perspective. *Urban For. Urban Green.* **2020**, *49*, 126630. [\[CrossRef\]](#)
14. Shah, A.; Garg, A.; Mishra, V. Quantifying the local cooling effects of urban green spaces: Evidence from Bengaluru, India. *Landsc. Urban Plan.* **2021**, *209*, 104043. [\[CrossRef\]](#)
15. Toparlar, Y.; Blocken, B.; Maiheu, B.; van Heijst, G.J.F. The effect of an urban park on the microclimate in its vicinity: A case study for Antwerp, Belgium. *Int. J. Climatol.* **2017**, *38*, e303–e322. [\[CrossRef\]](#)
16. Yan, H.; Wu, F.; Dong, L. Influence of a large urban park on the local urban thermal environment. *Sci. Total Environ.* **2018**, *622–623*, 882–891. [\[CrossRef\]](#)
17. Ren, Z.B.; He, X.Y.; Zheng, H.F.; Zhang, D.; Yu, X.Y.; Shen, G.Q.; Guo, R.C. Estimation of the Relationship between Urban Park Characteristics and Park Cool Island Intensity by Remote Sensing Data and Field Measurement. *Forests* **2013**, *4*, 868–886. [\[CrossRef\]](#)
18. Yu, C.; Hien, W.N. Thermal benefits of city parks. *Energy Build.* **2006**, *38*, 105–120. [\[CrossRef\]](#)
19. Lee, S.-H.; Lee, K.-S.; Jin, W.-C.; Song, H.-K. Effect of an urban park on air temperature differences in a central business district area. *Landsc. Ecol. Eng.* **2009**, *5*, 183–191. [\[CrossRef\]](#)
20. Zhang, Q.; Zhou, D.; Xu, D.; Rogora, A. Correlation between cooling effect of green space and surrounding urban spatial form: Evidence from 36 urban green spaces. *Build. Environ.* **2022**, *222*, 109375. [\[CrossRef\]](#)
21. Wang, P.; Yang, Y.; Ji, C.; Huang, L. Positivity and difference of influence of built environment around urban park on building energy consumption. *Sustain. Cities Soc.* **2023**, *89*, 104321. [\[CrossRef\]](#)

22. Han, Q.; Nan, X.; Wang, H.; Hu, Y.; Bao, Z.; Yan, H. Optimizing the Surrounding Building Configuration to Improve the Cooling Ability of Urban Parks on Surrounding Neighborhoods. *Atmosphere* **2023**, *14*, 914. [CrossRef]
23. Zhu, Z.; Zhou, D.; Wang, Y.; Ma, D.; Meng, X. Assessment of urban surface and canopy cooling strategies in high-rise residential communities. *J. Clean. Prod.* **2021**, *288*, 125599. [CrossRef]
24. Zhang, X.; Wang, Y.; Zhou, D.; Yang, C.; An, H.; Teng, T. Comparison of Summer Outdoor Thermal Environment Optimization Strategies in Different Residential Districts in Xi'an, China. *Buildings* **2022**, *12*, 1332.
25. Zhang, P.F. Spatial fluctuation of urban architecture. *J. Arid Resour. Environ.* **2016**, *30*, 51–57. [CrossRef]
26. Ministry of Housing and Urban-Rural Development, PRC. Design Standard for Thermal Environment of Urban Residential Areas (JGJ286—2013). 2013. Available online: [https://www.mohurd.gov.cn/gongkai/zhengce/zhengcefilelib/201309/20130926\\_224855.html](https://www.mohurd.gov.cn/gongkai/zhengce/zhengcefilelib/201309/20130926_224855.html) (accessed on 21 November 2023).
27. Yearbook, Xi'an Bureau of Statistics. Xi'an Statistical Yearbook, 2018. 2018. Available online: <http://tjj.xa.gov.cn/tjnj/2018/zk/indexch.htm> (accessed on 21 November 2023).
28. Liu, Z.N.; Yin, X.J. Urban Heat Island Effect and Meteorologic Factors in Xi'an. *J. Arid Land Resour. Environ.* **2008**, *22*, 87–90.
29. Lyu, Y. Research on the Cool Island Effect and Influencing Mechanism of Urban Green Space Based on Remote Sensing Data: Taking Xi'an as an Example. Master's Thesis, Xi'an Jiaotong University, Xi'an, China, 2022.
30. Kolokotsa, D.; Lilli, K.; Gobakis, K.; Mavrigiannaki, A.; Haddad, S.; Garshasbi, S.; Mohajer, H.R.H.; Paolini, R.; Vasilakopoulou, K.; Bartesaghi, C.; et al. Analyzing the Impact of Urban Planning and Building Typologies in Urban Heat Island Mitigation. *Buildings* **2022**, *12*, 537. [CrossRef]
31. Ge, J.; Wang, Y.; Zhou, D.; Gu, Z.; Meng, X. Building energy demand of urban blocks in Xi'an, China: Impacts of high-rises and vertical meteorological pattern. *Build. Environ.* **2023**, *244*, 110749. [CrossRef]
32. Lu, J.; Li, Q.; Zeng, L.; Chen, J.; Liu, G.; Li, Y.; Li, W.; Huang, K. A micro-climatic study on cooling effect of an urban park in a hot and humid climate. *Sustain. Cities Soc.* **2017**, *32*, 513–522. [CrossRef]
33. Spronken-Smith, R.A.; Oke, T.R. The thermal regime of urban parks in two cities with different summer climates. *Int. J. Remote Sens.* **2010**, *19*, 2085–2104. [CrossRef]
34. Hamada, S.; Ohta, T. Seasonal variations in the cooling effect of urban green areas on surrounding urban areas. *Urban For. Urban Green.* **2010**, *9*, 15–24. [CrossRef]

**Disclaimer/Publisher's Note:** The statements, opinions and data contained in all publications are solely those of the individual author(s) and contributor(s) and not of MDPI and/or the editor(s). MDPI and/or the editor(s) disclaim responsibility for any injury to people or property resulting from any ideas, methods, instructions or products referred to in the content.